# Temperature dependence of effective fluctuation time scales in spin glasses

G. G. Kenning,[1] J. Bowen,[2] P. Sibani,[3] and G. F. Rodriguez[2]
[1]*Department of Physics, Indiana University of Pennsylvania, Indiana, Pennsylvania 15705-1098, USA*
[2]*Department of Physics, University of California, Riverside, California 92521-0101, USA*
[3]*Institut for Fysik og Kemi, SDU, DK5230 Odense M., Denmark*
(Received 2 June 2009; revised manuscript received 5 December 2009; published 29 January 2010)

Using a series of fast-cooling protocols we have probed aging effects in the spin-glass state as a function of temperature. Analyzing the logarithmic decay found at very long-time scales within a simple phenomenological barrier model leads to the extraction of an effective fluctuation time scale of the system at a particular temperature. This is the smallest dynamical time-scale defining a lower cutoff in a hierarchical description of the dynamics. We find that this fluctuation time scale, which is approximately equal to atomic spin-fluctuation time scales near the transition temperature, follows a generalized Arrhenius law. We discuss the hypothesis that, upon cooling to a measuring temperature within the spin-glass state, there is a range of dynamically inequivalent configurations in which the system can be trapped, and check within a numerical barrier model simulation, that this leads to subaging behavior in scaling aged thermoremanent magnetization decay curves, as recently discussed theoretically [P. Sibani and G. G. Kenning, Phys. Rev. E **81**, 011108 (2010)].

DOI: 10.1103/PhysRevB.81.014424 PACS number(s): 75.50.Lk, 72.80.Ng, 71.55.Jv

## I. INTRODUCTION

Systems far from equilibrium display a range of interesting properties that are similar for what appear to be very different situations. Spin glasses are prototypical nonequilibrium systems that provide an interesting and accessible vehicle for the investigation of nonequilibrium statistical mechanics. Among the most striking properties of spin glasses are the time-dependent dynamics. Measuring time-dependent variations in the magnetization, as a function of temperature within the spin-glass state, allows a probe of accessible phase space. This phase space is characterized by highly degenerate, but distant, free-energy minima. In previous studies, many similarities have been found for measurements over a wide range of temperatures. For example, aging occurs at all temperatures below $T_g$, the spin-glass transition temperature.[1–3] The aged data, at different temperatures, also have some differences which, although subtle, require further study. These nonequilibrium properties are directly related to the underlying phase- and real-space structures of the system.

The dynamics of complex systems are known to depend strongly on the initial conditions,[4–6] defined as the state of the sample at the time the experiment begins, i.e., $t=0$ s at the beginning of the isothermal aging process or alternatively at the end of the quench. For spin glasses, the initial conditions depend on the thermal history occurring in the relatively short-time period starting when the sample temperature crosses $T_g$ and ending when the measurement temperature $T_m$ is reached. We report in this paper aging measurements using the thermoremanent-magnetization (TRM) decay for a range of measuring temperatures below $T_g$. The decay is measured at times $t>t_w$, where $t_w$ is the waiting time, defined as the interval between the time when the sample reaches the measuring temperature, $T_m$, and the time when the magnetic field, in which the sample is cooled through the transition temperature, is cut to zero. The observation time $t_{obs}=t-t_w$ is the time during which the data are taken. This quantity is traditionally called $t$ and is used an independent time variable for TRM measurements.

In a previous paper[7] we found, using a fast-quench-cooling protocol with "zero additional waiting time" (ZTRM), that the ZTRM decay showed a fairly standard TRM-like decay with a small effective waiting time ($\approx$19 s) which was associated with the cooling protocol. After several thousand seconds however, the ZTRM became logarithmic in time out to $10^5$ s, the longest time measured. Repeating the same procedure, but adding a short waiting time after the zero waiting time protocol, the $t_w$ dependent part of the decay ended at a time significantly longer than that found from the zero waiting time protocol but nevertheless ultimately decayed into the very same logarithmic time dependence. Subtraction of this logarithmic term from the long waiting time TRM decays (where scaling holds) utterly destroys the ability to scale the decay curves, implying that the logarithmic decay is not an additive term. These two empirical findings suggest that the states associated with the logarithmic decay are not an independent contribution to the magnetization decay but are intrinsic to the aging curves themselves. It was also shown that a hierarchical barrier model simulation with a uniform initial-state distribution produced a series of TRM decays (for different waiting times) that decayed into a common waiting time-independent logarithmic decay. The same conclusion was reached in a theoretical model[8] where the disappearance of the $t_w$ dependence of the TRM decay and subaging behavior result from heterogeneity of the initial configuration. The concept of spatial heterogeneity with a distribution of time scales is not new. Chamberlin[9] has observed nonresonant spectral hole burning in an AuFe(5%) spin-glass sample. He found that the decay observed after applying large-amplitude low-frequency magnetic fields implies a distribution of relaxation times corresponding to a heterogeneous system composed of many domains, each with its own characteristic temporal behavior. Montanari and Ricci-Tersenghi[10] have applied microscopic fluctuation dissipation relations to a given disorder realization of a highly frustrated ferromagnetic Ising model.

 

They find that single spins can exhibit heterogeneity of time scales. In this paper we apply the concept of heterogeneity to the barrier model of spin glasses through the imposition of an initial distribution of states with each state corresponding to an independent domain.

Numerical studies of multivalley energy landscapes of complex model systems, including Edward-Anderson spin glasses,[11–13] have charted out the "shape" of landscape valleys, i.e., regions of phase-space enclosing local energy minima. Defining for convenience the energy of a specific local minimum to be zero, the number of microscopic configurations $\mathcal{D}(E)$ within an interval of width $dE$ around energy $E$ was evaluated by exhaustive enumeration and other techniques. In most cases, this so-called local density of states has, for a range of $E$ values, a near exponential growth as a function of $E$, i.e., $\mathcal{D}(E) \approx c \exp(E/E_0)$, where $c$ and $E_0$ are constants. The parameter $E_0$ has the role of a local "transition temperature:" for $T > E_0$, the valley in question is not thermally accessible since the large number of configurations near its rim creates a "top heavy" Boltzmann quasiequilibrium distribution. In this regime, the thermalization process roams freely through the states near the rim of the valley. When $T < E_0$, the valley begins to act as a trap, as the configurations of low energy then carry a large probability. Interestingly, the values found numerically for $E_0$ for the Edwards-Anderson spin glass are close to the critical temperature of the model.[12,14] The numerical results just described were obtained for models of relative small size, and are applicable to the localized and bounded regions of a spin glass which are in a state of local thermal equilibrium, i.e., thermalized domains well known from numerical investigations.[15] Assuming that spatially bounded regions with a near exponential local density of state exist in a spin glass, a dynamical "phase transition" occurs as the temperature decreases below the transition temperature, whereby a hierarchically structured barrier space emerges for the volume. At the end of the quench, and the beginning of the isothermal aging process, several domains will be formed, each characterized by a maximum barrier. The system as whole is then characterized by an initial barrier distribution, which underlies the spatial heterogeneity of the system. Within each domain, the current configuration will be trapped in the hierarchy at a position mirroring the random configuration of the system right above the transition and hence a position which appears random in relation to the hierarchical barrier structure. It is plausible that this process repeats itself as the temperature is lowered leading to a continuum of phase transitions as the temperature decreases. The free-energy barriers within the space are strongly temperature dependent increasing rapidly in size as the temperature is lowered in the spin-glass phase. As the temperature decreases large barriers grow very large, effectively making regions of phase space inaccessible to each other while smaller barriers grow and replace larger barriers maintaining the hierarchical structure at each temperature. These barriers grow very fast as the temperature is reduced. For example, if we apply the relationship derived in Lederman *et al.*[16] [Eq. 8, using their values for the reduced temperature coefficients a and b] to our sample at $0.83T_o/T_g$ (26 K) we find that a reduction in temperature of $\Delta T \approx 0.1K$ is sufficient to increase the small barrier, associated with the cooling process, to a barrier size larger than the large barrier, associated with the time at which the TRM vanishes in isothermal aging at $T_m$. Hence, a portion of phase space which essentially looks flat at $T_m + \Delta T$ develops a full hierarchy of barriers when cooled to $T_m$. As the temperature decreases from $T_m + \Delta T$ to $T$, the state gets trapped in some valley of the barrier space and can migrate out of this portion of the space only if the surrounding barriers never grow larger than the barriers associated with the cooling time scale. As the measuring temperature is approached the barrier space at that particular temperature unfolds and within a single-particle picture the system enters and occupies a single state within the barrier space. There is no *a priori* reason for the occupation of any particular initial state other than the constraints due to growing barriers presented in the above arguments. In a large system composed of many volume limited independent domains, the initial-state occupations of each domain, would on average be random producing a uniformly distributed averaged initial state, leading to a logarithmic decay for $t \gg t_w$.[7,8] If the fluctuation time scale of the system is small and the time for hopping over the largest adjacent barrier associated with that particular state (i.e., the local barriers confining the state) is much less than the waiting time then full aging follows. If time for hopping over the smallest adjacent barrier is much greater than the waiting time then the state is effectively frozen and no aging would be observed. These states would however decay for measuring times $t \gg t_w$.

In Sec. II, we report TRM measurements made at a series of temperatures below $T_g$. In Sec. III we reanalyze the temperature-dependent ZTRM decays obtained[7] using rapid cooling protocols at a series of temperatures below the spin-glass transition temperature $T_g$. Finally we use the experimental results of Secs. II and III to determine parameters used to produce a series of barrier-model simulations of the temperature-dependent TRM decays. We then compare the scaling behavior of the experimental and simulation data.

## II. TEMPERATURE-DEPENDENT TRM DATA

In a previous paper[5] the results of various temperature-quenching protocols were reported at $T = 26$ K or $T_r = 0.83T_g$ for $Cu_{0.94}Mn_{0.06}$. We now examine other measurement temperatures. Previous studies[1–3] using conventional cooling techniques, have found the scaling parameter $\mu$ (determined by scaling the data with an effective waiting time $t_w^{\mu}$) to be relatively constant (approximately $\mu = 0.9$) over the temperature range $0.4T_g - 0.9T_g$. Outside of this temperature range, $\mu$ decreases. We have repeated our decay experiments (using similar fast-cooling protocols) at the same waiting times as before but now at different temperatures in order to examine the temperature-dependent behavior under more controlled conditions.

Starting from the same high temperature, $T_h = 35$ K, the sample is then rapidly cooled through the transition temperature $T_g = 31.5$ K to a measuring temperature $T_m$. At any particular measuring temperature a full range of TRM experiments were performed with waiting times ranging from 50 to 10 000s. Four different measuring temperatures were ex-

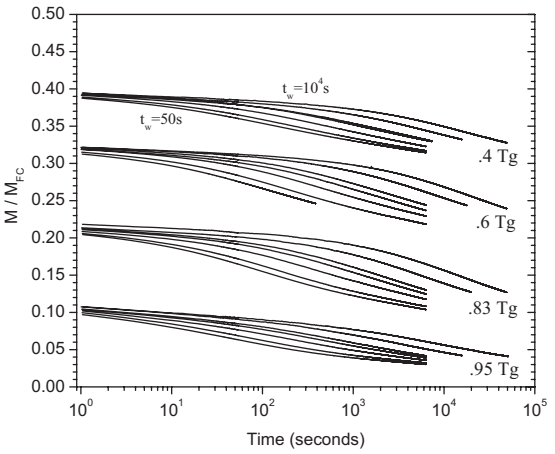


FIG. 1. Experimental TRM curves of $Cu_{0.94}Mn_{0.06}$ using fast-cooling protocols at four different temperatures. Each set of decay curves at given temperature display TRM decays for waiting times of $t_w$=50, 100, 300, 630, 1000, 3600, and 10 000 s. In each series the 50 s curve is the bottom curve and the magnetization increases systematically for increasing waiting time to the uppermost 10 000 s curve. The time on the $x$ axis begins after the magnetic field is cutoff.

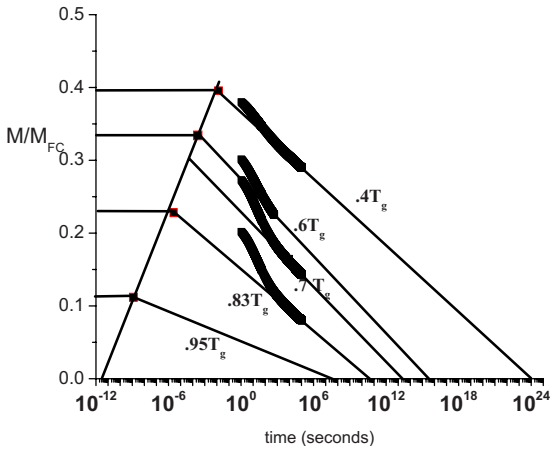


FIG. 2. (Color online) Fit of normalized ZTRM curves. The horizontal lines correspond to the value of $M_o$ determined from Fig. 1. The time on the $x$ axis begins after the magnetic field is cutoff. The $0.6T_g$ data we did not have a $10^5$ s ZTRM curve. A reasonable logarithmic extrapolation from a shorter time measurement was obtained by observing the systematic trend in the slope of the logarithm from a nearby $10^5$ s ZTRM curve at $0.7T_g$. The straight-line fit to the $0.95T_g$ data is from Ref. 5 (data lost). TRM decays were not measured at $0.7T_g$ so no $M_o$ value is implied.

plored: $T_m$=12.6, 18.9, 28.9, and 29.9 K, corresponding to reduced temperatures units $T_r=T_m/T_g$=0.4, 0.6, 0.9, and 0.95, respectively. The effective cooling times for the new temperatures are similar to the fast-cooling protocol employed for the $0.83T_g$ study (i.e., $t_c^{eff} \approx 20$ s). The cooling rate was however increased from 1 to 2 K/s for the lower temperatures.

Figure 1 shows the thermoremanent-magnetization-decay curves for different temperatures spanning the range of temperatures we probed. It can be observed, as has previously been observed[2] that there are qualitative similarities for aging data at different temperatures. There are however several significant differences. To begin with, the width of the decays (over the entire span of waiting times) for the two sets of data on the outer temperature ranges, $0.95T_g - 0.4T_g$, is slightly smaller than the width of the decays for the temperatures in the intermediate region. For all of the decays, at a particular measuring temperature, the magnetization values at the observation time of .5 s are similar but show a small increase as the waiting time increases. The curves then separate and at very long times appear as if they are going to come back together. In a previous paper[7] we showed that the curves actually recombine, within experimental observation times, for very short waiting times ($t_w \leq 45$ s). For the waiting times used in this study, the recombination of the long waiting-time curves is clearly outside of experimental measuring times. A second and more obvious difference is the magnitude of the initial remanence for each temperature. Assuming similar behavior for all of the temperatures the increased remanence suggests that, as the temperature is lowered, the logarithmic term would extend over a much longer time scale and make up a significantly larger proportion of the total remanence. For the high-temperature data the aged term is the majority of the remanence.

## III. ANALYSIS OF ZTRM CURVES

We start by reanalyzing some previously published data.[7] Figure 2 is a plot of ZTRM decays measured out to $10^5$ s for four temperatures and out to $10^3$ s for one temperature, i.e., $T=0.6T_g$. This data shows a long-time logarithmic tail from approximately $6\times10^3$ s out to $1\times10^5$ s for each of the temperatures (excluding $0.6T_g$). This tail appears to begin after the $t_w$ dependence of the cooling protocol comes to an end. Within the barrier model[7] we observe this behavior of aging decay giving way to a logarithmic decay when a uniform distribution is utilized. The extrapolation of the logarithmic term to zero magnetization is an intriguing result. The uniform distribution within the barrier model suggests that aging can occur with waiting times at least up to a maximum time, $\tau_{max}$, which is associated with the maximum barrier setup during the cooling process. Aging may still occur after this time if the domains and hence the barrier space continues to grow during the aging time. If the waiting time is significantly less than the maximum time then the aging curves will eventually decay into a common logarithmic decay. This result implies that even though time scaling may occur in the usual aging regime, time scaling eventually breaks down as the logarithmic decay is entered.

We continue with a natural extension of this analysis. In experimental ZTRM or TRM experiments, the cooling protocol imposes its own aging. Therefore the experiments never start with a pure nonaged distribution of states. It is well known from Field-Cooled/Zero-Field-Cooled (FC/ZFC) magnetization experiments that the remnant behavior is very large at low temperatures and decreases to zero at the transition temperature. It is within this remanence that aging behavior is observed. A TRM experiment begins by cooling the sample through the transition temperature along the field-

cooled curve and then, after waiting a time $t_w$, the field is dropped to zero. There is a rapid decrease in the magnetization due to the stationary magnetization decay. The stationary term is large and rapid with most of the decay occurring well before the measuring time begins in TRM measurements. The magnitude of the stationary term can be observed in Fig. 1. Before the TRM decay begins, there is an approximately 60% drop in the Field Cooled (FC) magnetization at $0.4T_g$ extending up to an approximately 90% drop in the FC magnetization at $0.95T_g$. If the stationary decay were instantaneous then the magnetization would drop from $M_{FC}$ to some value $M_o$ after which aging would then proceed. One can get a reasonably good estimate of $M_o$ from the TRM data displayed in Fig. 1. The $t_w=10^4$ s waiting-time curve is quite flat in the short-time regime. There is a slight slope in this time regime but it is likely that a portion of this is due to the effects of the stationary term. A reasonably good estimate of $M_o$ can therefore be found from a magnetization value just slightly greater than the shortest time value of the $10^4$ s TRM decay. This is the estimated value of the magnetization at which aging begins. The question can then be asked "what is the time scale at which aging begins." While, experimentally we cannot produce an idealized starting state after the quench, a uniform distribution within the barrier model offers a direction. If we began with a uniform distribution and looked at the decay with $t_w=0$ s we would find that the decay would be logarithmic starting at a time associated with the smallest barrier. The time for hopping over this smallest barrier is effectively the fluctuation time of the system at any particular temperature. In Fig. 2 we extrapolate the logarithmic term through short-time scales to the estimated value of the initial magnetization $M_o$. This was done for all temperatures at which we had a reasonable value of $M_o$. The fluctuation time at each temperature is read out as the intersection point of the corresponding curve. Remarkably these fluctuation times can be well fit by a straight line on a log-linear plot, i.e., by an Arrhenius function

$$\tau = \tau_o \exp\frac{E_a}{k_b T}. \tag{1}$$

The extrapolation of the line fit to the fluctuation times (Fig. 2), to zero magnetization, produces an effective fluctuation time scale at the transition temperature. The value obtained of $\tau_o \approx 3\times 10^{-12}$ s corresponds to time scales that might be expected for atomic fluctuations. A rapidly changing fluctuation time scale, as a function of temperature, coupled with the continuum of time scales associated with the barrier space could explain the glassy dynamics associated with the spin-glass phase.[17] At this point, the relationship between this minimum effective time scale for the aging component and critical fluctuations is unclear.

Within this simple model, we are arguing that each domain has a large distribution of time scales (represented by a hierarchical barrier structure) and heterogeneity, at a particular temperature, is determined by the initial starting-time scale for a particular domain. The onset of the phase transition is implied by ergodicity breaking and therefore diffusion within a hierarchical barrier space describes aging dynamics. In Fig. 2 it can be observed that $\tau_{max}$ (as well as $\tau_o$) decrease as the transition temperature is approached. It will be interesting to observe whether this difference between the maximum time and the fluctuation time vanishes at the transition temperature (i.e., $\tau_{max}-\tau_o \to 0$ s as $T \to T_g$). If this occurs, then as the temperature is lowered through the transition temperature, the spin-glass state would appear to evolve (in temporal range) continuously out of the paramagnetic phase. This type of continuous and subtle transition would help explain the lack of any observed discontinuity in the specific heat, at the transition temperature. At this stage, this type of transition is only a conjecture and clearly in need of further experimentation.

## IV. SIMULATIONS

In this section we perform barrier-model simulations using experimentally determined parameters. In general, the barrier model has four parameters. The first parameter $\alpha$ determines the linear growth rate of the barriers as a function of Hamming distance and is effectively the size of the smallest barrier. This parameter therefore also defines a minimum or fluctuation time scale $\tau_o$. The second parameter $N$ is the number of significant barriers in the system where $N\alpha$ is the size of the largest barrier and defines $\tau_{max}$. The third parameter $r$ is related to the branching ratio and the final parameter is the value of the initial magnetization, $M_o$. For more details of the barrier model, see Ref. 18. In the Appendix we show that there is a large region of $\alpha$ and $r$ over which simulated TRM experiments exhibit behavior similar to real systems. For this study we have chosen values of $\alpha=0.4$ and $r=1.15$. These values were picked somewhat arbitrarily from the range of values which exhibit proper diffusion behavior (Fig. 5) but were mainly chosen because diffusion on the time-scale probed occurs over several hundred barriers. Once $r$ and $\alpha$ were chosen, $N$ was chosen so that $\tau_{max}$ coincided with the maximum time found from the extrapolation of the experimental logarithmic term to zero magnetization. This also has the effect of setting the fluctuation time scale $\tau_o$. Finally, the integrated value of the uniform barrier distribution was set to $M_o$. Figure 3 displays the simulated TRM plots with the experimental parameters.

We can see from Fig. 3 that the barrier model gives a reasonably accurate representation of the experimental data. There are some significant differences however and some important similarities. One important difference between Figs. 3 and 1 is that the experimental data in the short-time regime has a slight slope to it whereas the simulations results, especially for the large waiting times, are fairly horizontal. Some of this difference may be due to the effect of the stationary term on the experimental data at short-time scales. A second important difference is that the range of simulated TRM decays appears to be slightly broader, for each temperature, than the range of the corresponding experimental data. There are also some interesting similarities. To begin with the set of waiting-time-dependent curves taken at the extreme temperatures $0.4T_g$ and $0.95T_g$. appear less broad over the range of waiting times then the intermediate temperatures $0.83T_g$ and $0.6T_g$. The similarities and differences are intriguing and we extend our analysis to include $\mu$

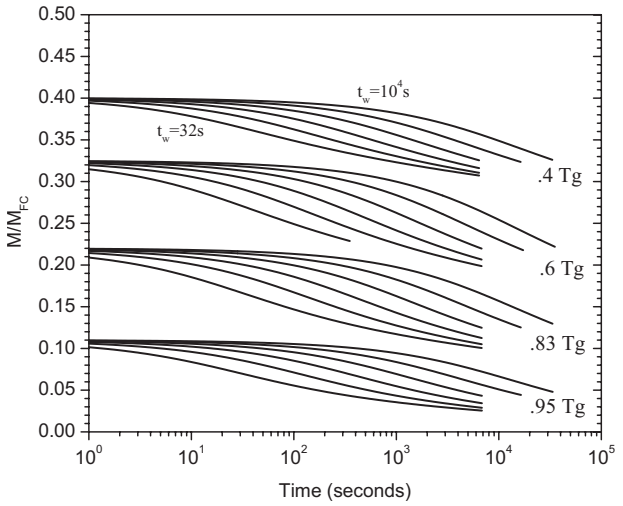


FIG. 3. Barrier-model simulation decays TRM decays of four different temperatures $0.4T_g$, $0.6T_g$, $0.83T_g$, and $0.95T_g$ using experimental parameters. Each set of decay curves at given temperature-display simulation TRM decays for waiting times of $t_w$=32, 100, 320, 1000, 3200, and 10 000 s. In each series the 32 s curve is the bottom curve and the magnetization increases systematically for increasing waiting time to the uppermost 10 000 s curve. The time on the $x$ axis begins after the magnetic field is cutoff.

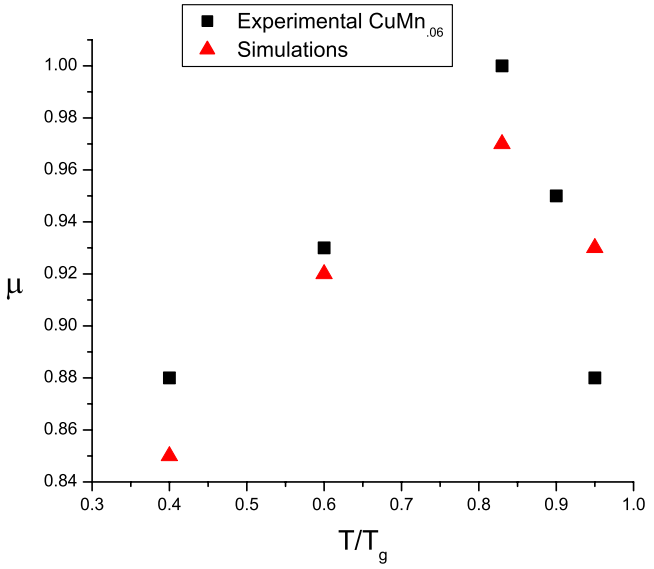


FIG. 4. (Color online) Best-fit $\mu$ values for various temperatures. The same eight $t_w$'s are used. The applied field is still 20 G. The measuring temperature is reached with the fast-cooling time protocols.

scaling of both the experimental and the simulation data to further probe the results. Scaling analyses for both the simulated and experimental data are presented in Fig. 4.

The experimental values of $\mu$, using the fast-cooling protocol, follow a similar pattern to those previously found in the original analyses of scaling behavior in spin glasses.[1,2] The $\mu$ values are however slightly higher at all temperatures. This result has previously been explained by Parker *et al.*[6] It is likely that the smaller $\mu$ values observed for the highest and lowest temperatures reflect the apparent narrowing of the decay set at $0.4T_g$ and $0.95T_g$. The implementation of $\mu$ scaling is somewhat subjective. It is clear that once the waiting-time-independent regime is reached (the logarithmic term), any type of waiting-time-dependent scaling will break down. Therefore neither the experimental or the simulation data can be scaled over the entire time range. The $\mu$ values determined from both experiment and simulations are found from scaling the largest waiting-time curves (as previously discussed[5]). The measuring-time region of the experimental data, obtained for large waiting-time regime, falls within the aging regime of the data and therefore reflects a situation similar to the previous implementations of this analysis. For experiment, the best $\mu$ value is obtained by scaling the time axis with a particular $\mu$ value and determining the best fit by eye. Using this technique, the best-fit parameter $\mu$ can be determined to an accuracy of approximately $\delta\mu \approx \pm 0.01$ for the entire temperature range excluding the highest temperature. For this temperature $\delta\mu \approx \pm 0.015$. Best-fit determination of $\mu$ for the simulation data provided reasonable scaling within a range of $\delta\mu \approx \pm 0.01$. One further comment on the scaling technique. As there was no noise intrinsic in the simulations we were able to analyze the scaling with much finer resolution than the experimental data. Observing the simulation curves with high resolution shows that perfect overlap of the curves does not hold for any $\mu$ value. These differences would be masked if noise was present. The finer points of implementation notwithstanding, $\mu$ scaling of the simulated data leads to several conclusions. Full aging ($\mu$ =1) was ruled out at all temperatures and subaging was observed. Since aging of an initial distribution concentrated on a single state leads to full aging, within the barrier model, we must conclude in agreement with Ref. 8, that subaging is a direct consequence of the distribution of states set up during the thermal quench. The similarities between the simulations and experiment are highly suggestive that heterogeneity is responsible for subaging in real systems.

## V. SUMMARY

In summary, we have measured the temperature-dependent TRM decay of CuMn(6%) using fast cooling protocols. We find that the fast-cooling protocols lead to $\mu$ scaling values larger than previously measured values. We have also reanalyzed the ZTRM data taken previously, at different temperatures, in conjunction with the TRM data reported in this paper. Extracting an initial starting magnetization $M_o$, from the TRM data, and extrapolating the apparent logarithmic long-time decay back to this initial magnetization allows us to determine a minimum-fluctuation time scale at any particular temperature. A plot of this time scale vs temperature produces apparent Arrhenius-type behavior. Extrapolation of this time scale to $M_o$=0 s corresponds to the fluctuation time scale at the transition temperature and appears to be approaching atomic-fluctuation time scales. The conjecture that cooling the spin glass through the transition temperature leads to a spatially heterogeneous distribution of fluctuation time scales provides an explanation for both the long-time "logarithmic" decay and subaging.

## ACKNOWLEDGMENTS

We would like to express great thanks to Ray Orbach for his support and useful discussions. We would also like to thank J. M. Hammann and M. Henkel for useful discussions.


## APPENDIX: SIMULATIONS ON THE BARRIER MODEL AND DETERMINATION OF BARRIER SPACE PARAMETERS

Using the Barrier Model, Joh *et al.*[18] have successfully simulated aging for a branching ratio (degeneracy factor) of $r=2$. It is still an open question as to what the value of the branching ratio actually is. Among the questions addressed in this appendix is whether the barrier model can successfully describe aging for systems with other branching ratios. What are the implications on the barrier space for a system with a smaller or larger branching ratio? Are there systematic relationships between the number of significant barriers and the branching ratio? Joh *et al.*[18] performed a series of calculations to model the zero-field cooled magnetization using a system with $n=20$ significant barriers to probe the parameters $r=2$ and $\alpha=2$. The significant barriers are those barriers which control diffusion within the model. With these parameters, the occupation of states for $t_w=10^3$, $10^4$, and $10^5$ (in units of attempt time), were contained within the first 20 significant barriers. They used a delta-function initial distribution located at the state associated with the lowest barrier for the initial distribution. It is generally believed that real experimental systems such as spin glasses have extremely large numbers of barriers. By varying the parameter $\alpha$, the slope of the significant barrier heights as a function of Hamming distance can be controlled. As the "slope" of the barriers heights decrease the diffusion of initial states can probe further and further into the barrier space. In this study we set out to probe much larger barrier spaces and the systems analyzed vary from 20 to 3000 significant barriers.

In traditional TRM/ZFC studies in spin glasses, a waiting time dependent magnetization decay is observed. An inflection point occurs at a time approximately equal to the waiting time and the function $S(t)=\frac{dM}{d\,\log(t)}$ exhibits a smooth single peak function with the peak occurring near the waiting time. Using the same initial distribution used by Joh *et al.* (i.e., a delta-function distribution located at the state associated with the lowest barrier) we have probed the parameter space $(\alpha,r)$ of the Barrier model. We find that for any particular value of $\alpha$, not all $r$ values give relaxations compatible with known experimental results. These results can be explained by looking at the terms in the transition matrix. The probability for occupation of a set of states at barrier $n$ is proportional to $r^n e^{-\alpha n}$. The occupation of states is dependent on two factors, $r^n$, the state degeneracy term at barrier $n$, and $e^{-\alpha n}$. For values of $r$ too large the degeneracy of states term tends to dominate the diffusion process and the states migrate more quickly to higher barriers; hence, $t_w^{eff}$ is larger for a given $t_w$. If $r$ is too small the states cluster at small barriers and hence a shoulder is observed in $S(t)$.

Using the criteria described above, we have determined that for a given value of $\alpha$ there is a finite interval of $r$ over which the experimental data can be qualitatively reproduced. In Fig. 5, we plot the parameter space of $r$, as a function of $\alpha$, that allows for $S(t)$ curves that reasonably reproduce experimental data. In general, this plot was produced by choosing a particular value of $\alpha$ and then probing the degeneracy factor $r$. Decay curves found within these boundaries exhibit full aging and the aging curves extend over the whole magnetization region (i.e., there is no logarithmic component). It should be pointed out that the values used by Joh *et al.*[18] ($r=2$ and $\alpha=2$) fall well within this region. We observe that as $\alpha$ decreases, the region, of acceptable branching-ratio parameters $r$ narrows significantly. Figure 5(b) extends the region of $\alpha$ down to $\alpha=0.02$. The system size at $\alpha=0.02$ probed out to approximately 3000 barriers. Qualitatively, Fig. 5(b) suggests that as $\alpha$ approaches a value of zero, $r$ appears to asymptotically approach a value of 1.

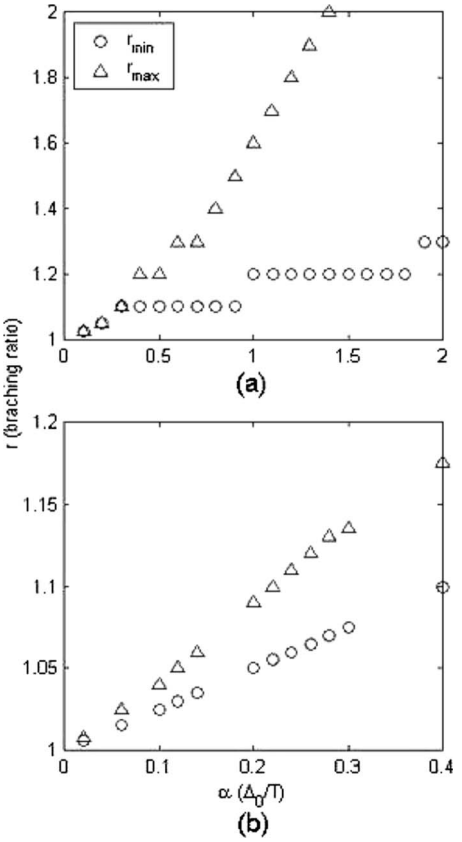


FIG. 5. Range of qualitative agreement with experimentally determined $S(t)$ curves. Open circles determine lower bound. Open triangles determine upper bound.

### Case I: Linearly increasing barrier height with Hamming distance

The asymptotic limits (i.e., $r=1$ as $\alpha\rightarrow 0$) can be explained in terms of maintaining an approximately constant number of states at a particular energy barrier even though $\alpha$ and $r$ may change. We will show that under a self-similarity condition, the degeneracy, $r$, approaches unity in the limit of $\alpha$ approaching zero. The self-similarity condition maintains that within the model similar behavior occurs on all size and

energy scales and that the only relevant parameter is the time $t_w$ under which the system is allowed to evolve. In particular, the change in the number of states at some energy barrier $N$ should be proportional to the change in barrier height at $N$. The proportionality constant is dependent only on $N$ and not on the relationship of the barrier height to the Hamming distance or other features of the manifold.

We define a general barrier density of states at barrier $N$ as

$$D(\Delta) = \frac{dn}{d\Delta}, \tag{A1}$$

where $n$ is the number of states at barrier $N$. Let us assume that for a given parameterization of the barrier space reasonable aging effects exist. For example, using parameters $\alpha_1$ and $r_1$ reasonable $S(t)$ curves are generated and the barrier density of states is centered on a most probable barrier number $N_1$. Using the approximation

$$\frac{dn}{d\Delta} \simeq \frac{\delta n}{\delta \Delta} \tag{A2}$$

it follows that

$$D(\Delta) = \frac{r^{N_1}}{\Delta_1} = k_B T \frac{r^{N_1}}{\alpha_1}, \tag{A3}$$

where $r^{N_1}$ is the number of states associated with significant barrier $N_1$ and $\Delta_1$ is the size of the energy increment between significant barriers.

Now consider a second system, at the same temperature, with barrier separation defined by $\alpha_2$, branching ratio $r_2$, and most probable barrier number $N_2$. Under the self-similarity condition we require that

$$D_1(\Delta_1) = D_2(\Delta_2) \tag{A4}$$

leading to

$$k_B T \frac{r^{N_1}}{\alpha_1} = k_B T \frac{r^{N_2}}{\alpha_2}. \tag{A5}$$

From this equation we obtain the expression

$$\ln(r_2) = \frac{N_1}{N_2} \ln(r_1) + \frac{1}{N_2} \ln\left(\frac{\alpha_1}{\alpha_2}\right). \tag{A6}$$

In the model, decreasing $\alpha_2$ has the effect of decreasing the slope of increase in the significant barriers. Therefore, during the waiting time, the initial state will diffuse over a larger number of significant barriers to reach the most probable barrier $N_2$. In the limit that $\alpha_2 \to 0$ the most probable barrier $N_2 \to \infty$. Therefore, under the condition $-\ln \alpha_2 < N_2$, as $\alpha_2 \to 0$ the value of the branching ratio $r_2 \to 1$.


[1] M. Ocio, M. Alba, and J. Hammann, J. Phys (Paris), Lett. **46**, L1101 (1985).

[2] M. Alba, M. Ocio, and J. Hammann, Europhys. Lett. **2**, 45 (1986).

[3] M. Alba, J. Hammann, M. Ocio, Ph. Refregier, and H. Bouchiat, J. Appl. Phys. **61**, 3683 (1987).

[4] V. S. Zotev, G. F. Rodriguez, G. G. Kenning, R. Orbach, E. Vincent, and J. Hammann, Phys. Rev. B **67**, 184422 (2003).

[5] G. F. Rodriguez, G. G. Kenning, and R. Orbach, Phys. Rev. Lett. **91**, 037203 (2003).

[6] D. Parker, François Ladieu, Jacques Hammann, and Eric Vincent, Phys. Rev. B **74**, 184432 (2006).

[7] G. G. Kenning, G. F. Rodriguez, and R. Orbach, Phys. Rev. Lett. **97**, 057201 (2006).

[8] P. Sibani and G. G. Kenning, Phys. Rev. E **81**, 011108 (2010).

[9] R. V. Chamberlin, Phys. Rev. Lett. **83**, 5134 (1999).

[10] A. Montanari and F. Ricci-Tersenghi, Phys. Rev. Lett. **90**, 017203 (2003).

[11] P. Sibani, C. Schön, P. Salamon, and J.-O. Andersson, Europhys. Lett. **22**, 479 (1993).

[12] P. Sibani and P. Schriver, Phys. Rev. B **49**, 6667 (1994).

[13] J. C. Schön and P. Sibani, Europhys. Lett. **49**, 196 (2000).

[14] P. Sibani, R. van der Pas, and J. C. Schön, Comput. Phys. Commun. **116**, 17 (1999).

[15] J. Kisker, L. Santen, M. Schreckenberg, and H. Rieger, Phys. Rev. B **53**, 6418 (1996).

[16] M. Lederman, R. Orbach, J. M. Hammann, M. Ocio, and E. Vincent, Phys. Rev. B **44**, 7403 (1991).

[17] See, for example, K. Binder and A. P. Young, Rev. Mod. Phys. **58**, 801 (1986) and references therein.

[18] Y. G. Joh, R. Orbach, and J. Hammann, Phys. Rev. Lett. **77**, 4648 (1996).